Nitric Oxide Potentiates Hydrogen Peroxide–induced Killing of *Escherichia coli*

By Roberto Pacelli,* David A. Wink,* John A. Cook,* Murali C. Krishna,* William DeGraff,* Norman Friedman,* Maria Tsokos,‡ Amram Samuni,§ and James B. Mitchell*

*From the *Radiation Biology Branch and ‡Laboratory of Pathology, National Cancer Institute, Bethesda, Maryland 20892-1002; and §Molecular Biology Department, Hebrew University Medical School, Jerusalem 91010, Israel*

Summary

Previously, we reported that nitric oxide (NO) provides significant protection to mammalian cells from the cytotoxic effects of hydrogen peroxide (H_2O_2). Murine neutrophils and activated macrophages, however, produce NO, H_2O_2, and other reactive oxygen species to kill microorganisms, which suggests a paradox. In this study, we treated bacteria (*Escherichia coli*) with NO and H_2O_2 for 30 min and found that exposure to NO resulted in minimal toxicity, but greatly potentiated (up to 1,000-fold) H_2O_2-mediated killing, as evaluated by a clonogenic assay. The combination of NO/H_2O_2 induced DNA double strand breaks in the bacterial genome, as shown by field-inverted gel electrophoresis, and this increased DNA damage may correlate with cell killing. NO was also shown to alter cellular respiration and decrease the concentration of the antioxidant glutathione to a residual level of 15–20% in bacterial cells. The iron chelator desferrioxamine did not stop the action of NO on respiration and glutathione decrease, yet it prevented the NO/H_2O_2 synergistic cytotoxicity, implicating metal ions as critical participants in the NO/H_2O_2 cytocidal mechanism. Our results suggest a possible mechanism of modulation of H_2O_2-mediated toxicity, and we propose a new key role in the antimicrobial macrophagic response for NO.

Nitric oxide (NO)[1] originates from the biotransformation of L-arginine to L-citrulline by nitric oxide synthase (NOS) (1). NOS is found in several different cells, including endothelia, neurons, and macrophages (2, 3). In murine macrophages, NOS is upregulated by cytokines such as IFN-γ, TNF-α, and LPS (4–6). When murine macrophages and neutrophils are activated by bacterial invasion of the host, they produce NO together with other reactive species ($O_2^-\cdot$, H_2O_2, ·OH, HOCl) (7). Presumably, because NO, H_2O_2, and $O_2^-\cdot$ are produced when macrophages and neutrophils are activated to kill pathogenic microorganisms, their simultaneous presence should provide an advantage to the host cell. A previous report postulated that the peroxynitrite ion formed by the reaction of NO with superoxide anion is, at least in part, responsible for macrophage-mediated bacteriocidal action (8). A more recent study showed that the spontaneous NO-releasing agent [$((C_2H_5)_2N[(O)NO]^-Na^+$), diethylamine (DEA)/NO] protects mammalian cells from the H_2O_2-induced cytotoxicity (9). An antagonistic interaction between NO and H_2O_2 is mechanistically intriguing since macrophages must themselves survive as well as protect normal surrounding mammalian cells while secreting toxic species to defend against bacteria. We therefore undertook studies to better define (*a*) whether NO plus H_2O_2 is bacteriocidal to *Escherichia coli*; (*b*) the potential mechanism(s) underlying the bacteriocidal effect; and (*c*) the critical cellular target for NO/H_2O_2–mediated damage. For these studies, DEA/NO was used as a NO donor agent. DEA/NO has a half-life of 2.5 min at 37°C and netural pH, and it spontaneously releases two equivalents of NO per mole (10). DEA/NO provides a means of delivering NO without the problems associated with the use of NO gas. Our studies show increased bacteriocidal action resulting from the combination of H_2O_2 and NO and describe our efforts to characterize the phenomenon.

[1]*Abbreviations used in this paper:* DEA, diethylamine; DF, desferrioxamine; FIGE, field inverted gel electrophoresis; GSH, glutathione; HX, hypoxanthine; LB, Luria-Bertani; NO, nitric oxide; NOS, nitric oxide synthase; NO_x, nitrogen oxide species; ONOO$^-$, peroxynitrite; ROS, reactive oxygen species; SOD, superoxide dismutase; XO, xanthine oxidase.

Materials and Methods

Hypoxanthine (HX), oxypurinol, Hepes buffer, superoxide dismutase (SOD) (Cu/Zn, Mn, and Fe), desferrioxamine (DF), DEA, sodium nitrite, glutathione, nicotinamide dinucleotide phos-

phate, glutathione peroxidase, hydrogen peroxide, diethylenetriaminopentaacetic acid, and lucigenin were purchased from Sigma Chemical Co. (St. Louis, MO); catalase and xanthine oxidase (XO) were purchased from Boehringer Mannheim Corp. (Indianapolis, IN). Agar and soft agar were purchased from GIBCO BRL (Gaithersburg, MD). Nitric oxide gas and nitrogen were purchased from Matheson Gas Products (East Rutherford, NJ). Argon came from M.G. Industries (Malvern, PA). PBS and Luria-Bertani (LB) medium were purchased from Quality Biological Inc. (Gaithersburg, MD). All water was distilled and subsequently purified further through a water purification system (Milli-Q; Millipore Corp., Bedford, MA). DEA/NO ($(C_2H_5)_2N[(O)NO]^-Na^+$) was provided as a generous gift from Joseph Saavedra (National Cancer Institute, Frederick, MD) (synthesized and purified as previously described [10]). A Bradford protein reagent kit was purchased from Bio-Rad Laboratories (Hercules, CA). The "v vials" used in the anaerobic experiments were purchased from Wheaton Industries (Millville, NJ). A spectrophotometer (model DU 65; Beckman Instruments, Inc., Fullerton, CA) was used for bacteria OD measurements. The *E. coli* strains JM 101, K-12 RW193, K-12 RW B19, and HB101 were obtained from American Type Culture Collection (Rockville, MD). The *E. coli* strains 1157, KL-16, and its *x*th A mutant were obtained from *E. coli* Genetic Stock Center (Yale University, New Haven, CT).

Cytotoxicity Assay. Bacteria were grown in LB medium in a shaker incubator, 250 revolutions/min, at 37°C until the cell density registered an absorbance at 600 nm of 0.2 (for the log phase assay) or 1.4 (for the plateau phase assay). The cells were suspended in 5 ml of PBS–20 mM Hepes buffer at a concentration of 10^6/ml and exposed for 30 min at 37°C to either different concentrations of H_2O_2 (0.1, 0.5, 1, and 2 mM) or 5 mM HX + 0.2 U/ml XO with or without DEA/NO (0.01, 0.1, and 1.0 mM). For control, 1 mM DEA and 1 mM sodium nitrite ($NaNO_2$) (end products after NO release from DEA/NO) were used instead of the DEA/NO, together or separately, in the presence of H_2O_2. Catalase (for H_2O_2) at a final concentration of 260 U/ml or catalase and oxypurinol (for HX/XO) at a final concentration of 0.1 mM were used to stop the reactions. After treatment, the cells were rinsed and diluted in PBS, and an aliquot of 0.5 ml (with the appropriate dilution to yield a scorable number of colonies on dishes) was plated in triplicate on LB agar plates and placed in a 37°C incubator in an air atmosphere. After an overnight incubation, the plates were removed, and the colonies were counted. All experiments were conducted a minimum of three times, and data points are in triplicate. The data shown in the figures are results from one of the triplicate experiments, and error bars (shown when larger than symbol) represent standard deviations. Linear regression and *t* test analyses as conducted in Fig. 2 *A* were performed using the program Systat 5.2 (SYSTAT Inc., Evanston, IL).

Some experiments were performed under hypoxic conditions by bubbling argon for 30 min into 2 ml of PBS bacteria suspension (10^6/ml) in a 5-ml v vial. The bacterial suspension was then exposed to either an argon-bubbled H_2O_2 (1 mM) or DEA/NO (1 mM) solution or to both for 30 min. The reactions were terminated by the addition of catalase, and the bacteria were plated as described above.

Experiments with DF were performed as follows. The bacteria ($5–10 \times 10^6$/ml) were grown for 2 h (OD at 600 nm = 0.15–0.25) in LB broth with DF (0.5 or 1 mM) at 37°C in the shaker incubator. The cells were then suspended in PBS–20 mM Hepes buffer with DF (1 mM) and treated with DEA/NO and H_2O_2 as described above.

For the NO gas experiments, LB medium–20 mM HEPES was bubbled for 30 min with nitrogen to remove oxygen, with NO for 1 h, and then stored in sealed glass bottles and used for the experiments with the cells and H_2O_2. The bacteria (10^6/ml) were suspended in the gassed media and incubated for 30 min with or without 1 mM H_2O_2. At the end of the experiment, catalase was added for 1 min, and then the bacteria were plated as described above. For the anoxic NO gas experiments, the bacteria were suspended (10^6/ml) in 2 ml PBS containing 20 mM Hepes in a 5-ml v-vial, and argon gas was bubbled into the solution for 5 min. Aliquots (2 ml) of anoxic bacterial suspension were then treated in three separate ways: (*a*) H_2O_2 solution (15 μl) was injected to produce a final concentration of 0.5 mM argon-bubbled H_2O_2; (*b*) 0.5 ml NO gas alone; and (*c*) both H_2O_2 and NO gas together. The treatment conditions were maintained for 20 min at 37°C, after which the samples were bubbled for 3 min with argon to remove any residual NO gas, and then the vials were opened and 4 μl of catalase (260 U/ml) was added. The bacteria were then plated as described above.

Cu/Zn SOD was used at concentration up to 5,000 U/ml in the cell toxicity experiments, and catalase was used at 260 U/ml. The enzymes were added before drug treatment.

SOD Activity Evaluation. The activity of the three different SOD isoenzymes (Cu/Zn, Fe, and Mn) was evaluated as described by McCord and Fridovich (11) after 30-min exposure to either H_2O_2 (0.1 or 1 mM) or DEA/NO (1 mM) or both.

In bacteria, the relative SOD activity was determined by measuring the loss of chemoluminescence produced from the reaction of superoxide anion ($O_2^- \cdot$) with lucigenin (12) when an aliquot of sonicated bacteria extract was added to the reaction. Chemoluminescence measurements were made using a spectrofluorometer (model 8000; SLM-Aminco, Urbana, IL), with a photomultiplier tube in the photon counting mode. The reaction mixture consisted of 50 mM phosphate buffer, pH 8.0, containing 5 mM HX, 200 μM lucigenin, 200 U/ml catalase, and 50 μM DTPA. Chemoluminescence was produced by the addition of 0.03 U/ml XO. After 3–5 min (to allow the light output to reach a plateau), 20 μl of the sonicated bacterial extract was added to the light-producing mixture. Counts before and after the addition of the bacterial extract were taken, and the percentage of loss of chemoluminescence was calculated. All treated samples were then compared with the light loss from the untreated control sample (as light intensity decreases, SOD inhibition increases). Bacterial extracts were also heated in boiling water for 1 h and tested for SOD activity; no SOD activity in these samples could be measured. The experiments were performed in triplicate.

Field-inverted Gel Electrophoresis (FIGE). Bacteria (10^7/ml) were treated as described above in LB broth, and the DNA was labeled by incubating the cells with 0.02 μCi/ml [^{14}C]thymidine for 2 h before and during the exposure. DNA was prepared for electrophoresis by the method of Schwartz and Cantor (13) as modified by Ager et al. (14) and Stamato and Denko (15). After treatment, the bacteria were resuspended in PBS at 10^9/ml. An equal volume of 2% low-melting-temperature agarose was added, and the cell suspension was drawn with a syringe into 3/32-in. (internal diameter) silicone tubing. Both ends of the tubing were clamped, and the tubing was immersed in an ice bath to solidify the agarose rapidly. The agarose was then extruded from the tubing and cut into 5-mm lengths; these "plugs" were placed into 1.5-ml centrifuge tubes. The cell wall was digested, incubating the plugs in 1 mg/ml lysozyme in TE buffer (10 mM Tris, 1 mM EDTA) for 1 h. DNA was released by incubating at 55°C in lysis buffer (Tris-NaCl, 1% sarkosyl, and 1 mg/ml proteinase K) for 24 h. The

plugs were then rinsed in TE buffer for 24 h with three buffer changes. RNA was digested by incubation with 0.1 μg/ml boiled RNase A in TE buffer for 2 h at 37°C.

The 0.8% agarose gels were cast in 0.5 × TBE (1 × TBE is 90 mM Tris, 90 mM boric acid, and 2.5 mM EDTA). Agarose plugs were loaded into 2 × 6 × 5–mm wells, which were sealed with melted agarose. Electrophoresis was performed for 24 h at 56 V (4 V/cm), with a 3:1 ratio of forward/reverse pulse time. The initial forward pulse time was 7.5 s (reverse pulse 2.5 s), increasing to a final forward pulse time of 90 s (final reverse pulse 30 s). The running buffer (0.5 × TBE) was recirculated and cooled to 12–15°C, as previously described by Stamato and Denko (15), to keep the released DNA concentrated in a narrow band to facilitate quantitation (see below). After electrophoresis, the gels were soaked in 0.5 μg/ml ethidium bromide for 30 min, destained for 30 min with distilled water, and photographed on a UV light box. The lanes were separated from one another, and the well containing the plug was separated from the portion of the lane containing the released DNA. These small pieces of agarose were put into separate scintillation vials, and, after adding 50 μl of concentrated HCl to prevent resolidification of the agarose, the agarose was melted by placing each vial on a hot plate. To each vial, 15 ml of Hydrofluor® (National Diagnostics Inc., Atlanta, GA) was added, and radioactivity was determined using a scintillation counter (model 1217; LKB Instruments, Bromma, Sweden). The data are expressed as a percentage of DNA remaining in the well and were calculated as follows:

$$\text{Percent of DNA remaining} = \frac{\text{CPM in the well}}{\text{CPM in the lane} + \text{CPM in the well}} \times 100.$$

Oximetry. Log phase bacteria were suspended (5×10^7) in LB medium and incubated with or without 1 mM DEA/NO at 37°C. After 15 min, an aliquot (2 ml) of each sample was tested for oxygen consumption using an oxygraph (model 5/6; Gilson Medical Electronics, Inc., Middleton, WI) equipped with a Clark-type electrode.

H_2O_2 Consumption. The levels of H_2O_2 in the presence of different bacterial cell concentrations were measured by spectrophotometrically monitoring the formation of I_3^- from I^- as previously described (16).

Glutathione (GSH) Measurements. For aerobic evaluation, log phase bacteria (10^8/ml) were incubated in 20 ml of LB broth in the presence of DEA/NO (1 mM) for 30 min and then pelleted and resuspended in 1 ml of 0.6% sulfosalicylic acid. For anoxic evaluation, 10 ml of LB bacteria suspension (200×10^6/ml) were bubbled for 1 h with argon and then treated with an argon-bubbled DEA/NO solution. After 30 min, the bacterial suspension was bubbled again with argon to remove all the NO, and the sealed vial was cooled to 4°C before opening. The amount of GSH was calculated by a modification of Tietze's method (17) and expressed in micrograms GSH/milligrams protein. Protein concentrations were assessed by the Bradford method (18). GSH levels were also measured in mammalian cells (Chinese hamster V79 lung fibroblasts). Log phase V79 cells were grown in F12 medium plus 10% FCS. Cells were treated with 1 mM DEA/NO for 30 min, and GSH levels were determined as described above.

Assays for Glutathione Peroxidase and Glutathione Transferase. Glutathione peroxidase activity was measured by following the decrease in reduced nicotinamide dinucleotide phosphate absorbance at 340 nm after the addition of 0.17 U/ml of human glutathione peroxidase isolated from human red blood cells (Sigma Chemical Co.), glutathione reductase and 1 mM H_2O_2. Glutathione transferase activity was measured by following absorbance changes at 340 nm using the transferase substrate chlorodinitrobenzene. The reaction mixture included 5 U/ml of the π human placental transferase (Sigma Chemical Co.) with 1 mM chlorodinitrobenzene and 1 mM GSH.

Electron Microscopy. Log phase bacteria (2×10^7/ml) were exposed for 30 min to 1 mM DEA/NO, 1 mM H_2O_2, or both. The cells were pelleted and fixed in 2.5% glutaraldehyde in phosphate buffer (pH 7.4) at room temperature for 24 h, postfixed in OsO_4, and embedded in Maraglas 655 (Ladd Research Industries Inc., Burlington, VT). Sections were stained with uranyl acetate–lead citrate and examined with an electron microscope (model 400; Philips Technologies, Cheshire, CT).

Results and Discussion

DEA/NO + HX/XO Cytotoxicity. Upon host invasion by bacteria, neutrophils and macrophages are activated and begin to consume oxygen rapidly (19). During this "oxygen burst," murine macrophage release, among other moieties, NO, $O_2^-\cdot$ and H_2O_2 (2, 7). To stimulate these conditions, we produced NO, $O_2^-\cdot$, and H_2O_2 in a continuous manner, as might be expected by bacterially activated macrophages. *E. coli* strain JM101 (20) was treated with DEA/NO that releases NO and/or HX/XO, which produces in an aerobic environment $O_2^-\cdot$ and H_2O_2. When these cells were exposed for 30 min to NO generated in situ from DEA/NO (0.01, 0.1, and 1 mM), minimal or no toxicity was observed. $O_2^-\cdot$ and H_2O_2 produced in situ enzymatically with HX/XO caused 50–90% cell killing. Using 1 mM DEA/NO in the presence of H_2O_2 and $O_2^-\cdot$, the cytotoxicity was enhanced by 10,000-fold (Fig. 1). Peroxynitrite ($ONOO^-$), the product of the reaction of $O_2^-\cdot$ with NO, has been implicated in the NO-mediated bacteriocidal effect of NO (8). We therefore tried to elucidate the actual species responsible for the DEA/NO bacteriocidal potentiation by removing either $O_2^-\cdot$ or H_2O_2 from the reaction.

SOD and Catalase Effects on Cytotoxicity. We attempted to eliminate $O_2^-\cdot$ from the reaction mixture by adding 5,000 U of Cu/Zn-SOD (~5 μM). Cu/Zn-SOD was not deactivated by NO (data not shown). Considering the concentration of NO and SOD as well as their respective rate constants of reaction with $O_2^-\cdot$ (21–23), 5,000 U/ml SOD should have been sufficient to compete effectively for $O_2^-\cdot$ and diminish the $ONOO^-$ formation. As is seen in Fig. 1, the addition of SOD did not decrease the DEA/NO potentiation. As further proof that extracellular $ONOO^-$ was not participating as an active intermediate in the observed potentiation, we placed catalase in the HX/XO mixture to remove all H_2O_2. In the absence of H_2O_2, where only NO, $O_2^-\cdot$, and potentially $ONOO^-$ would be formed, no potentiation was observed (Fig. 1). The failure of SOD and the success of catalase to prevent the DEA/NO cytotoxicity only exclude $O_2^-\cdot$ and by extension $ONOO^-$ anion from having importance extracellularly but do not rule out the possibility that $ONOO^-$ anion may still function as a key toxic intermediate intracellularly.

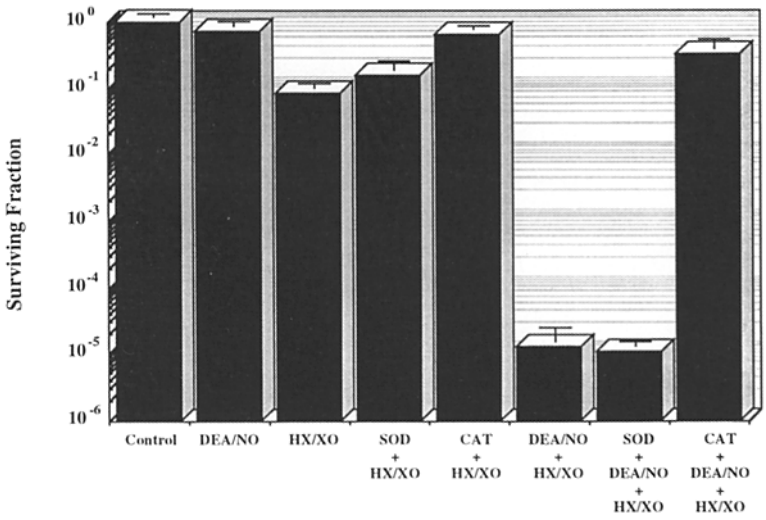

Figure 1. Survival of *E. coli* (JM 101 cells) treated for 30 min with DEA/NO (1.0 mM), HX (0.5 mM)/XO (0.2 U/ml), SOD (200 U/ml) + HX/XO catalase (*CAT*) (260 U/ml) + HX/XO, DEA/NO + HX/XO, SOD + DEA/NO + HX/XO, and CAT + DEA/NO + HX/XO.

If intracellular $O_2^{-}\cdot$ were elevated, it is conceivable that the different response to NO/H_2O_2 exposure in mammalian cells compared with *E. coli* may result from the bacteria having different isoforms of SOD that are susceptible to inactivation by the NO/H_2O_2. Bacterial cells contain Fe-SOD, possibly trace quantities of periplasmic Cu/Zn-SOD, and an oxygen-inducible Mn-SOD (24, 25), whereas mammalian cells have Cu/Zn cytoplasmicallly and Mn-SOD intramitochondrially (24). Therefore, the three purified isoforms of SOD were treated in vitro individually for 30 min with DEA/NO (1 mM) and H_2O_2 (1 mM). DEA/NO plus H_2O_2 or H_2O_2 alone inactivated the Fe-SOD but not the other isoforms (data not shown). To test whether the endogenous Fe-SOD was inactivated, JM 101 cells were treated with H_2O_2 plus DEA/NO, then the cell lysate was assayed for total SOD activity. The treated cells lost ~50% of the SOD activity found in untreated cells (Table 1). These results do not allow us to categorically conclude that the loss in SOD activity alters the sensitivity of the cells to an experimental oxidative stress. However, we decided to simplify the experimental system by removing $O_2^{-}\cdot$ from the extracellular reaction conditions by using only H_2O_2 and DEA/NO.

DEA/NO + H_2O_2 Cytotoxicity. Treatment of *E. coli* with bolus H_2O_2 (0.1, 0.5, 1, and 2 mM) for 30 min resulted in cell killing between 10 and 90% (Fig. 2 *A*). When DEA/NO and H_2O_2 were applied simultaneously, the results were similar to those obtained with HX/XO; DEA/NO potentiated toxicity in a concentration-dependent manner (Fig. 2 *A*). To confirm that it was indeed the NO generated from DEA/NO that potentiated H_2O_2 cytotoxicity and not the decomposition products of DEA/NO, cells were treated with H_2O_2 and the decomposition products of DEA/NO (sodium nitrite and diethylamine). As seen in Fig. 2 *B*, only intact DEA/NO potentiated the cytocidal effects of H_2O_2, whereas the decomposition products did not. An additional experiment was conducted to rule out the possible contribution of metabolically generated $O_2^{-}\cdot$ to the H_2O_2 potentiation by DEA/NO by treating cells with H_2O_2 under hypoxic conditions. As shown in Fig. 3 *A*, H_2O_2 cytotoxicity was also enhanced under hypoxic conditions by DEA/NO treatment. To eliminate any possibility that a DEA/NO decomposition intermediate was responsible for the observed potentiation, we conducted a further experiment using NO gas in combination with H_2O_2, as described in Materials and Methods. As shown in Fig. 3 *B*, potentiation of H_2O_2 cytotoxicity by NO gas treatment was also observed. Collectively, these results not only implicate the role of NO in the potentiation but support our use of DEA/NO as an NO delivery compound.

Table 1. *Total SOD Activity of JM 101 Cells Treated with H_2O_2 ± DEA/NO*

Condition	Relative percent of SOD activity
Control	100 ± 11
1 mM DEA/NO	63 ± 1
1 mM H_2O_2	96 ± 2
1 mM H_2O_2 + 1 mM DEA/NO	32 ± 7

To assure ourselves that these results were not specific for JM 101 cells, we tested the combination of NO and H_2O_2 in five other *E. coli* strains. In all cases, *E. coli* were synergistically killed by the combination of NO and H_2O_2 (Fig. 4). Likewise, we examined the effects of cell density at the time of H_2O_2 exposure for JM 101 cells. Over a cell density range from 10^6 to 10^8/ml, potentiation of H_2O_2 cytotoxicity was observed that was similar to the potentiation observed in Fig. 2 *A* (data not shown).

To determine whether bacterial cells had to be actively dividing and metabolizing for there to be potentiation between NO and H_2O_2, plateau phase cells were compared with those in exponential growth. Potentiation of plateau phase cells was observed with the combination of DEA/NO and H_2O_2 (Fig. 5), but the cytotoxicity was decreased

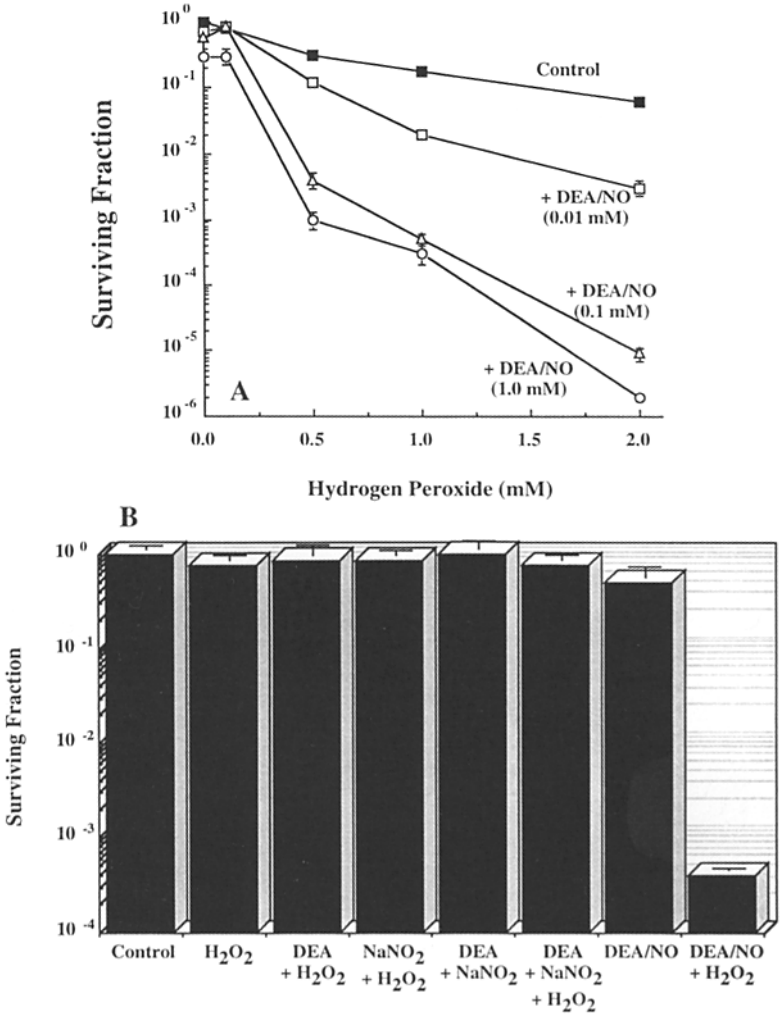

Figure 2. (*A*) Survival of *E. coli* treated with various concentrations of H_2O_2 for 30 min in the absence or presence of DEA/NO (0.01, 0.1, or 1 mM). The data presented are from a single representative experiment. Data from three replicate experiments were pooled, and Student's *t* tests were conducted to determine statistical significance of the difference between the different treatments. Linear regression was performed on each dose–representive curve. The differences in derived slopes of the H_2O_2 alone and the various DEA/NO concentrtations plus H_2O_2 were then evaulated by *t* test analysis. Compared with H_2O_2 alone, the *P* values for DEA/NO treatment were as follows: 0.1 mM DEA/NO, $P = 0.0028$; 0.5 mM DEA/NO, $P = 0.0017$; and 1.0 mM DEA/NO, $P = 0.0016$. (*B*) Survival of *E. coli* treated wth H_2O_2 (1 mM) for 30 min in the absence or presence of the decomposition products of DEA/NO (1 mM), DEA, and nitrite ($NaNO_2$).

compared with the exponentially growing cultures, presumably because of a decreased metabolism rate of plateau phase cells. To elucidate further the requirements of the bacterial potentiation, we examined whether both reagents must be present simultaneously, or if NO or H_2O_2 alone cause a lasting cellular dysfunction that is unmasked by the other agent. To this end, bacteria were first exposed to either DEA/NO (1 mM) for 30 min and then H_2O_2 (1 mM), or first to H_2O_2 (1 mM) for 30 min followed by a 1-min incubation with catalase to remove any residual unmetabolized H_2O_2 and then DEA/NO (1 mM). In neither case was potentiation observed (data not shown). The H_2O_2 concentration was monitored to determine the H_2O_2 consumption during the 30-min exposure. When cell densities of $\geq 10^8$ cells/ml were used, the H_2O_2 levels were quickly depleted; however, below 10^7 cells/ml, no significant depletion of H_2O_2 levels was observed (Fig. 6 *A*).

Oxygen Consumption. It has been reported that NO may interfere with respiration (26), which may in part explain the different effect NO has on peroxide-mediated cytotoxicity in bacterial and mammalian cells. Clark electrode oximetry showed that NO profoundly decreases oxygen utilization by *E. coli* (Fig. 6 *B*) and suggested that this may be a cause of the observed potentiation. NO itself reacts with oxygen to form other nitrogen oxide species (NO_x), which have been argued to be important in biological toxicities. These reactive NO_x have been shown to modify DNA chemically and to inhibit various enzymes (27–31). Therefore, elevated intracellular levels of oxygen could result in the formation of reactive NO_x. However, as noted above, when bacteria were treated with H_2O_2 in a hypoxic environment, there was potentiation by DEA/NO (Fig. 3). We cannot rule out the possibility that oxygen is produced during catalase metabolism of H_2O_2 and, therefore, cannot absolutely exclude that oxygen functions in some manner to increase potentiation between NO and H_2O_2. However, the hypoxic experiments do suggest a minor role in the potentiation for NO_x and $ONOO^-$.

Effect of Metal Chelators on Cytotoxicity. Numerous examples suggest that H_2O_2 is not cytotoxic until reduced by either Fe^{+2} or Cu^{+1} ions to yield either ·OH or hypervalent metal ions (19). Previous reports have shown that iron and other metal ions may be released from sulfide–iron clusters or sulfhydryl–iron chelates when treated with NO (31). If NO were responsible for releasing intracellular redox-active iron during H_2O_2 treatment, and this were a

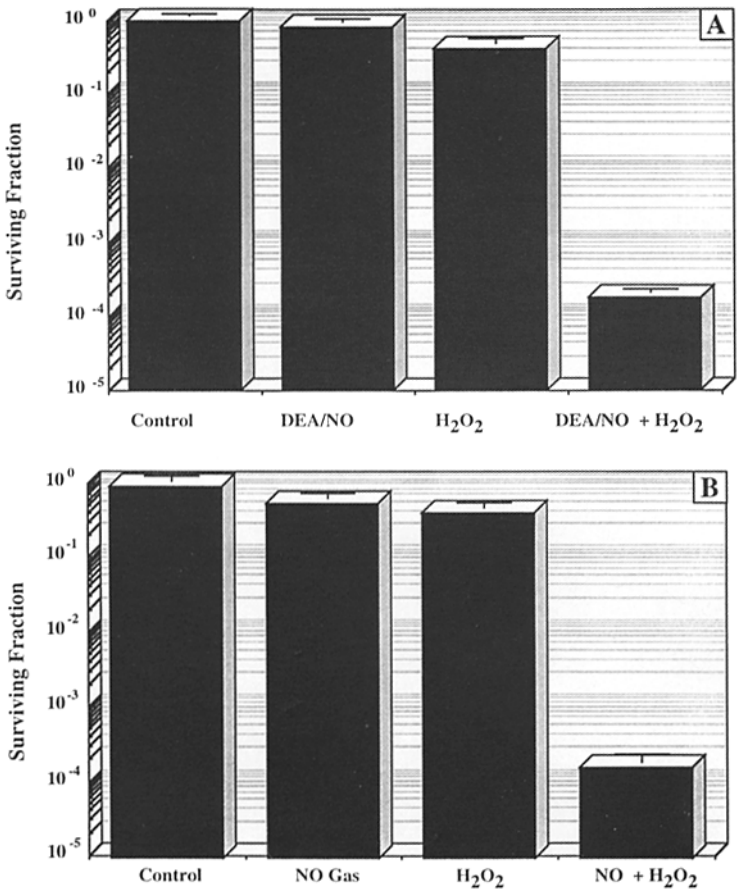

Figure 3. Surival of *E. coli* treated with DEA/NO alone (1 mM), H_2O_2 alone (1 mM), or DEA/NO + H_2O_2 for 30 min under hypoxic conditions. (*B*) Survival of *E. coli* treated with NO gas alone, H_2O_2 alone (1 mM), or NO gas + H_2O_2 for 30 min under hypoxic conditions.

mechanism involved in the observed synergy, then chelation of the redox-active iron released by NO should eliminate the observed potentiation. This hypothesis was tested by preincubating cells with the iron-chelating agent DF for varying times to allow time for sequestration of mobilized intracellular iron ions. After incubation, the cells were treated with DEA/NO plus H_2O_2. Fig. 7 demonstrates that DF preincubation for 2 hr eliminated the potentiating effect of DEA/NO plus H_2O_2. Furthermore, when cells were not preincubated with the chelator, and DF was present only during the treatment, the potentiating toxicity was not affected. The lack of protection in this last condition indicates that the potentiation may result from redox-active iron ion being released intracellularly. Furthermore, DF did not interfere with NO-induced ablation of respiration (Fig. 6 *C*). This is evidence that DF can protect against cytotoxicity without restoring oxygen consumption and, therefore, rules out the possibility that DF is reacting directly with NO or some of its bioproducts as previously proposed (see Fig. 6, *B* and *C*) (32). Therefore, we conclude that DF must be protecting by chelating transition metals, particularly iron ion, and as a corollary the observed potentiation is mediated, at least in part, by transition metal ions.

The protective effect of DF excludes the possibility that

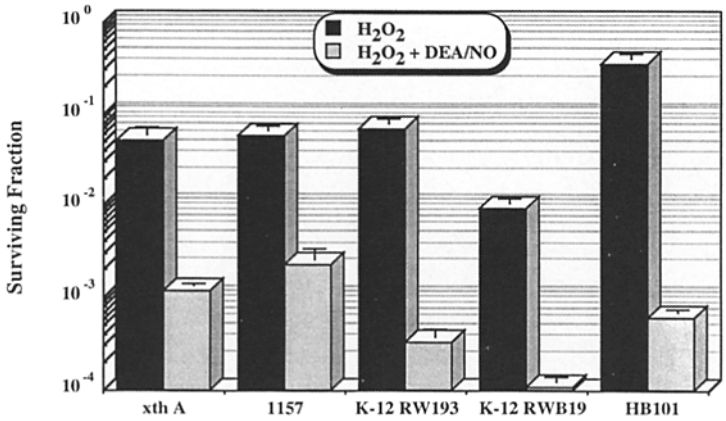

Figure 4. Survival of five different strains of *E. coli* treated in an aerobic environment with H_2O_2 (1 mM) in the absence or presence of DEA/DO (1 mM). For these studies, the different strains were treated identically, as seen in Fig. 2 *B*.

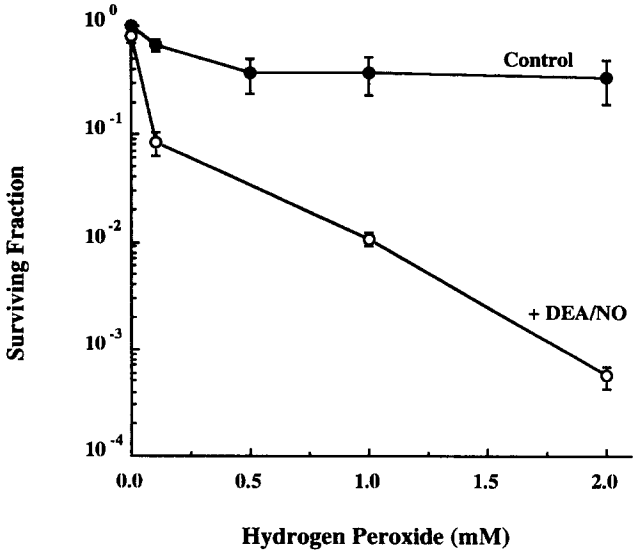

Figure 5. Survival of plateau phase *E. coli* treated with varying concentrations of H_2O_2 in the absence (●) or presence (○) of DEA/NO (1 mM) for 30 min under aerobic conditions.

the NO/H_2O_2 potentiation results by releasing iron and inactivating metal-containing enzymes, such as aconitase (33, 34) or DNA repair enzymes (30, 35). Had NO inactivated such enzymes by iron release, the enzymes would remain inactivated by NO even in the presence of DF. DF reacts to chelate adventitious Fe^{3+} ions; it does not stop NO from releasing iron from sulfur–iron clusters. Therefore, NO may still inactivate respiration in the presence of DF, as is seen in Fig. 6 *B*. DF would tightly bind adventitious Fe^{3+} ions and thereby prevent formation of Fe^{2+} and stop the subsequent reaction with H_2O_2 to produce highly oxidizing species that may damage critical cellular targets such as DNA (36).

Molecular Target of DEA/NO + H_2O_2 Cytotoxicity. To delineate further how DEA/NO enhances H_2O_2 damage, we treated the cells with DEA/NO and either *t*-butyl hydroperoxide or cumene hydroperoxide—two agents known to cause oxidation of lipid membranes (37, 38). DEA/NO did not potentiate the oxidative effect of either agent (data not shown). Electron microscopy was used to ascertain if there was gross damage to the bacterial cell wall/membrane by DEA/NO and H_2O_2. No such damage was noted (data not shown). Our inability to demonstrate membrane damage by electron microscopic evaluation does not rule out more subtle disruption of the membrane function. However, the results do not support the hypothesis that bacterial protoplasmic membrane is the organelle structure damaged by the combination of DEA/NO and H_2O_2.

Because H_2O_2 is known not to cause observable double-strand breaks of genomic DNA (15), we performed FIGE (13–15) on JM 101 cells to ascertain if NO altered the effect of H_2O_2 on bacterial genomic DNA double-strand breaks. Table 2 shows that treatment with H_2O_2 does not result in observable double-strand scissions beyond that found in non-H_2O_2–treated cells (87.7 vs. 85.9% undamaged DNA). However, when DEA/NO is present during the H_2O_2 exposure, an increased number of double-strand DNA breaks is observed (26.9 vs. 87.7% undamaged DNA). To be consistent with survival studies performed with JM

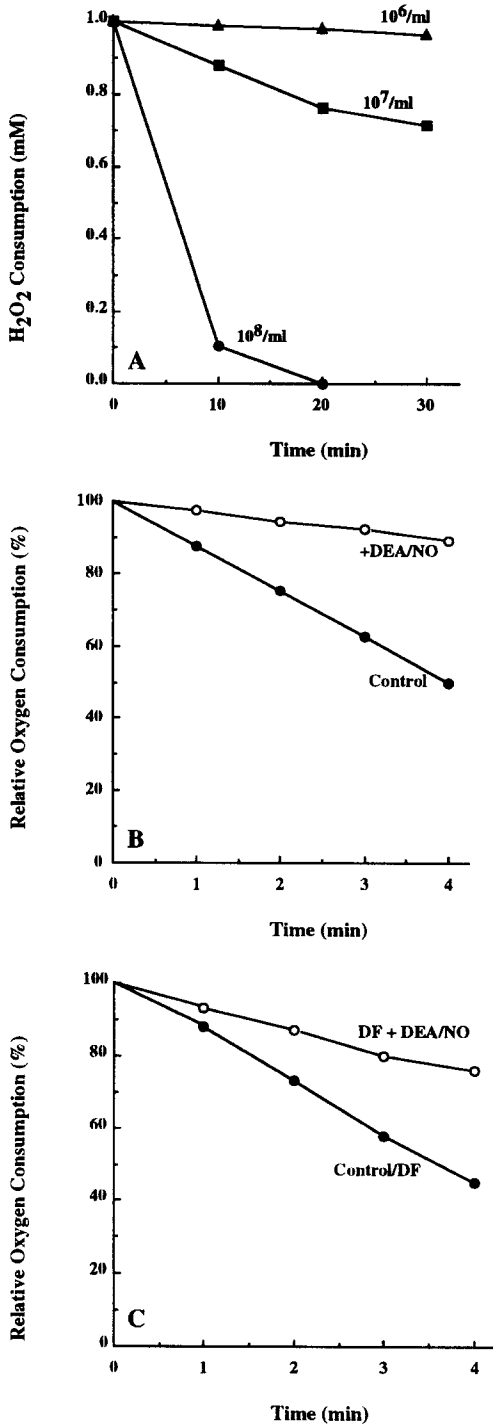

Figure 6. (*A*) H_2O_2 consumption at different cell densities of JM 101 cells as a function of time at 37°C. (*B*) Oxygen consumption of JM 101 cells in the absence or presence of DEA/NO (1 mM) as a function of time at 37°C. (*C*) Oxygen consumption of JM 101 cells pretreated with 1 mM DF in the absence or presence of DEA/NO (1 mM) as a function of time at 37°C.

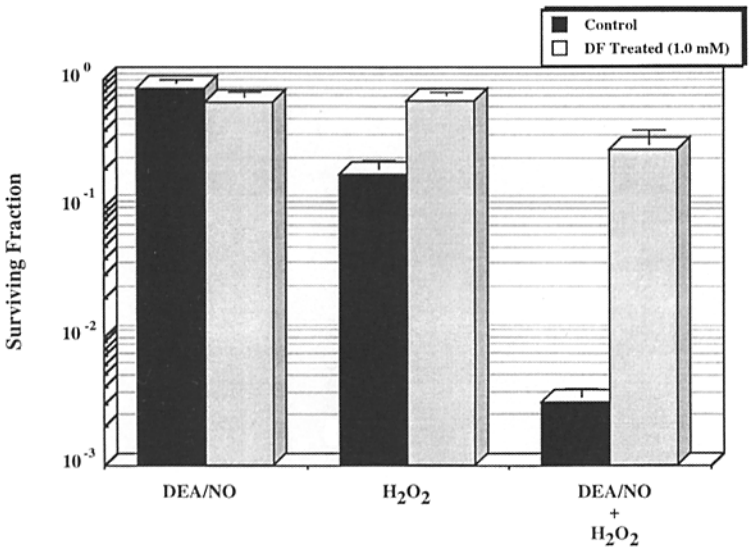

Figure 7. Survival of *E. coli* exposed to DEA/NO (1 mM) ± DF (1 mM); H_2O_2 (1 mM) ± DF (1 mM); or DEA/NO + H_2O_2 ± DF (1 mM) for 30 min. Cultures were pretreated with DF 2 h before and during H_2O_2 exposure. ■, Control; □, DF treated (1 mM).

Table 2. *DNA Double-stranded Break for H_2O_2 ± DEA/NO*

Control	DEA/NO	H_2O_2	DEA/NO + H_2O_2
DF (−) 85.9	87.0	87.7	26.9
DF (+) 86.6	89.9	90.4	63.9

The numbers represent the percentage of DNA that was not damaged and are the expression of the intact genomic DNA that was in the well of the FIGE. *DF(−)*, without DF; *DF(+)*, with DF at 0.5 mM.

101 cells, DF, which provided substantial protection of *E. coli* from DEA/NO/H_2O_2, should protect *E. coli* against these double-strand breaks. Table 2 demonstrates that DF treatment does indeed protect *E. coli* (63.9% undamaged DNA) from DEA/NO/H_2O_2 double-strand break induction when compared with the non-DF–treated cells (26.9%). As noted, protection was not complete because DF did not restore the DNA to the level of the DF/H_2O_2 treatment (90.4%).

Because GSH is known to be an important detoxifier of H_2O_2 (39) and metal complexes of NO can react with GSH (31), we examined whether intracellular GSH was depleted by treatment with DEA/NO in both V79 cells (mammalian cells that NO protected against H_2O_2 [9]) and JM 101 cells. DEA/NO decreased the intracellular GSH levels in mammalian cells by only 35%, whereas in JM 101 cells, intracellular GSH levels decreased by 75–85% (Table 3). Decreasing the intracellular GSH levels by 75–85% of control during an oxidative stress may well contribute to the bacteriocidal potentiation from NO and H_2O_2. We tested some of the enzymes in which GSH is a cofactor and found that DEA/NO does not inactivate GSH peroxidase or GSH transferase (data not shown).

Conclusions. In summary, our data illustrate the following points regarding the release of NO during an oxidative burst: (*a*) NO potentiated the bacteriocidal effect of H_2O_2; (*b*) a target of the potentiation appears to be DNA; (*c*) superoxide, $ONOO^-$, or NO_x species seem to have a minor role in the potentiation; (*d*) transition metal ions are involved in the synergistic cytotoxicity; and (*e*) GSH levels are decreased by DEA/NO. These findings suggest that the enhancement of H_2O_2-induced DNA strand scission and cytotoxicity by NO may be due to several factors, as depicted in Fig. 8.

Fig. 8 illustrates that in *E. coli*, the respiratory enzyme complexes are found within the inner membrane of the cell envelope (40). In a normal oxygen environment, the respiratory enzymes probably consume the majority of oxygen arriving at the bacterial inner membrane, as depicted by step I in Fig. 8. Hence, the concentration of oxygen that reaches the cytoplasm is low, and the portion that does enter into the cell is more than likely reduced to superoxide,

Table 3. *GSH (μg/mg protein) in Four Different E. coli Strains and Chinese Hamster V79 Cells Treated with 1 mM DEA/NO*

Strain	JM 101	KL-16	1157	9101 *xth*	V79 cells
Control	12.14	16.52	40.80	13.72	10.2
+ DEA/NO	1.54 (87%)*	3.44 (79%)	18.12 (56%)	2.20 (84%)	6.6 (35%)

The bacteria strains and the mammalian cell line (V79) were treated and assayed as described in Materials and Methods.
*The percentages in brackets represent depletion of GSH by DEA/NO.

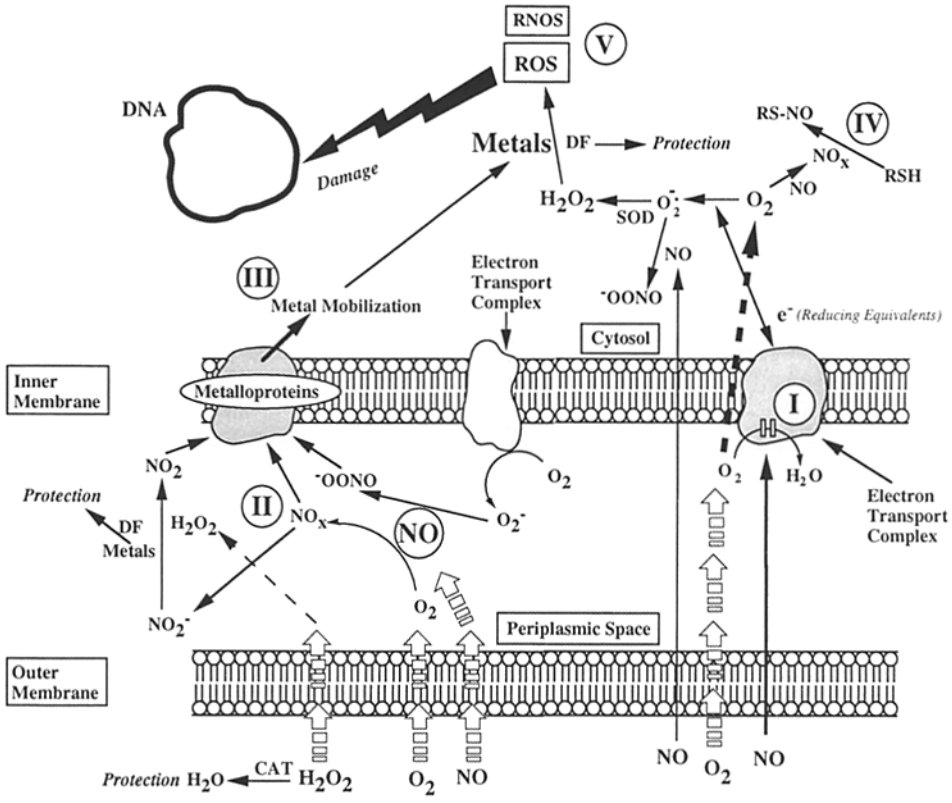

Figure 8. Proposed interactions between NO and ROS to mediate bacterial cytotoxicity in the periplasmic space and cytosol of bacteria. Circled numbers indicate potential cellular sites where NO may enhance H_2O_2 cytotoxicity. (*I*) NO interferes with electron transport and thereby allows more oxygen to enter the cytosol, thus making available reducing equivalents for superoxide production. (*II*) Production of NO_x in the periplasmic space, which has potential to react with metalloproteins and form nitrites. (*III*) Release of redox-active metals from metalloproteins by NO and nitrogen oxide–derived species. (*IV*) Reaction of NO_x with sulfhydryl functional groups of proteins and nonproteins. This reaction would interfere with the detoxification of H_2O_2 by GSH-dependent pathways. (*V*) Production of ROS and/or reactive nitrogen oxide species (*RNOS*) with subsequent damage to DNA.

which would be detoxified by the two isoforms of SOD. We have shown that oxygen consumption by JM 101 cells is almost completely stopped by NO (Fig. 6 *B*). Inhibition of oxygen consumption should allow more oxygen to cross into the intracytoplasmic space and form high levels of the superoxide anion, as denoted by a bold, dashed arrow in Fig. 8. Diminution of GSH would then result from the reaction of NO_x and RSH (cellular thiols) compounds (Fig. 8, *step IV*), (41) which would permit Fenton reactions to produce reactive oxygen species (ROS) (Fig. 8, *step V*) that would go on to oxidatively damage intracellular targets. Fenton reactions should accelerate as a result of NO-induced release of labile, redox-active transition metals (Fig. 8, *step III*). Such an increase should result in more DNA damage, and ultimately this would lead to the enhanced cytotoxicity that we have observed in the JM 101 cells. Metal mobilization (Fig. 8, *step III*) and increased intracellular iron have been shown to facilitate both cell killing and DNA damage by H_2O_2 (42). Previous studies implicated NO in the bactericidal activity of macrophages, since inhibition of NOS greatly reduced cytotoxicity (43–45). Lastly, it is known that nonheme iron proteins (Fig. 8, *step II*) are in greater abundance in bacteria than in mammalian cells and as such may be a ready source for iron mobilization as well as deactivation by NO. Iron–sulfur proteins such as aconitase are particularly sensitive to damage by reactive nitrogen oxide species (Fig. 8, *step II*) (34, 46, 47), which would then result not only in enzymic deactivation but also in an increased cytoplasmic low-molecular-weight, redox-active iron pool. Were redox-labile iron ions to occur in the near vicinity of bacterial DNA, damage to DNA would be expected to be more facile (Fig. 8, *step V*). In mammalian cells, enzymes such as aconitase are not in close proximity to DNA. The differences in compartmentalization and the higher amount of iron–sulfur proteins in bacteria compared with mammalian cells appear to explain the different response to oxidative stress.

The differential response of mammalian cells (9) and bacteria to NO/H_2O_2 may afford a unique means to combat invading microorganism invasion with minimal damage to host cells. Our results provide a framework to better understand how the production of NO can enhance the immune response to *E. coli* invasion and yet limit toxicity to the host cells.

Address correspondence to Dr. James B. Mitchell, Radiation Biology Branch, Building 10, Room B3-B69, National Cancer Institute, National Institutes of Health, 9000 Rockville Pike, Bethesda, MD 20892-1002.

Received for publication 23 March 1995 and in revised form 26 June 1995.

References

1. Ignarro, L.J. 1990. Biosynthesis and metabolism of endothelium-derived nitric oxide. *Annu. Rev. Pharmacol. Toxicol.* 30: 535–560.
2. Nathan, C. 1992. Nitric oxide as a secretory product of mammalian cells. *FASEB J.* 6:3051–3064.
3. Moncada, S., R.M.J. Palmer, and E.A. Higgs. 1991. Nitric oxide: physiology, pathophysiology, and pharmacology. *Pharmacol. Rev.* 43:109–142.
4. Ding, A.H., C.F. Nathan, and D.J. Stuehr. 1988. Release of reactive nitrogen intermediates and reactive oxygen intermediates from mouse peritoneal macrophages. Comparison of activating cytokines and evidence for independent production. *J. Immunol.* 141:2047–2412.
5. Xie, Q.W., H.J. Cho, J. Calaycay, R.A. Mumford, K.M. Swiderek, T.D. Lee, A. Ding, T. Troso, and C. Nathan. 1992. Cloning and characterization of inducible nitric oxide synthase from mouse macrophages. *Science (Wash. DC).* 256: 225–228.
6. Lyons, C.R., G.J. Orloff, and J.M. Cunningham. 1992. Molecular cloning and functional expression of an inducible nitric oxide synthase from a murine macrophage cell line. *J. Biol. Chem.* 267:6370–6374.
7. Nathan, C.F. 1987. Secretory products of macrophages. *J. Clin. Invest.* 79:319–326.
8. Zhu, L., C. Gunn, and J.S. Beckman. 1992. Bactericidal activity of peroxynitrite. *Arch. Biochem. Biophys.* 298:452–457.
9. Wink, D.A., I. Hanbauer, M.C. Krishna, W. DeGraff, J. Gamson, and J.B. Mitchell. 1993. Nitric oxide protects against cellular damage and cytotoxicity from reactive oxygen species. *Proc. Natl. Acad. Sci. USA.* 90:9813–9817.
10. Maragos, C.M., D. Morley, D.A. Wink, T.M. Dunams, J.E. Saavedra, A. Hoffman, A.A. Bove, L. Isaac, J.A. Hrabie, and L.K. Keefer. 1991. Complexes of NO with nucleophiles as agents for the controlled biological release of nitric oxide. Vasorelaxant effects. *J. Med. Chem.* 34:3242–3247.
11. McCord, J.M., and I. Fridovich. 1969. Superoxide dismutase. An enzymatic function for erythrocuprein (hemocuprein). *J. Biol. Chem.* 244:6049–6055.
12. Faulkner, K., and I. Fridovich. 1993. Luminol and lucigenin as detectors for $O_2^{-\cdot}$. *Free Radic. Biol. Med.* 15:447–451.
13. Schwartz, D., and C. Cantor. 1984. Separation of yeast chromosomes by pulsed field gradient electrophoresis. *Cell.* 37: 67–75.
14. Ager, D.D., W.C. Dewey, K. Gardiner, W. Harvey, R.T. Johnson, and C.A. Waldren. 1990. Measurement of radiation-induced DNA double-strand breaks by pulsed field gel electrophoresis. *Radiat. Res.* 122:181–187.
15. Stamato, T.D., and N. Denko. 1990. Asymmetric field inversion gel electrophoresis: a new method for detecting DNA double-strand breaks in mammalian cells. *Radiat. Res.* 121: 196–205.
16. Hochanadel, C.J. 1952. Effects of cobalt gamma-radiation on water and aqueous solutions. *J. Phys. Chem.* 56:587–594.
17. Tietze, F. 1969. Enzymic method for quantitative determination of nanogram amounts of total and oxidized glutathione: applications to mammalian blood and other tissues. *Anal. Biochem.* 27:502–522.
18. Bradford, M.M. 1976. A rapid and sensitive method for the quantitation of microgram quantities of protein utilizing the principle of protein-dye binding. *Anal. Biochem.* 72:248–254.
19. Clifford, D.P., and J.E. Repine. 1982. Hydrogen peroxide mediated killing of bacteria. *Mol. Cell. Biochem.* 49:143–149.
20. Messing, J., R. Crea, and P.H. Seeburg. 1981. A system for shotgun DNA sequencing. *Nucleic. Acids Res.* 9:309–321.
21. Huie, R.E., and S. Padmaja. 1993. The reaction of NO with superoxide. *Free Radic. Res. Commun.* 18:195–199.
22. Beckman, J.S., J. Chen, H. Ischiropoulos, and J.P. Crow. 1994. Oxidative chemistry of peroxynitrite. *Methods Enzymol.* 233:229–240.
23. Koppenol, W.H., J.J. Moreno, W.A. Pryor, H. Ischiropoulos, and J.S. Beckman. 1992. Peroxynitrite, a cloaked oxidant formed by nitric oxide and superoxide. *Chem. Res. Toxicol.* 5: 834–842.
24. Beyer, W., J. Imlay, and I. Fridovich. 1991. Superoxide dismutases. *Prog. Nucleic Acid Res. Mol. Biol.* 40:221–253.
25. Benov, L.T., and I. Fridovich. 1994. *Escherichia coli* express a copper- and zinc-containing superoxide dismutase. *J. Biol. Chem.* 269:25310–25314.
26. Geng, Y.J., A.S. Petersson, A. Wennmalm, and G.K. Hansson. 1994. Cytokine-induced expression of nitric oxide synthase results in nitrosylation of heme and nonheme iron proteins in vascular smooth muscle cells. *Exp. Cell Res.* 214:418–428.
27. Wink, D.A., K.S. Kasprzak, C.M. Maragos, R.K. Elespuru, M. Misra, T.M. Dunams, T.A. Cebula, W.H. Koch, A.W. Andrews, and J.S. Allen. 1991. DNA deaminating ability and genotoxicity of nitric oxide and its progenitors. *Science (Wash. DC).* 254:1001–1003.
28. Nguyen, T., D. Brunson, C.L. Crespi, B.W. Penman, J.S. Wishnok, and S.R. Tannenbaum. 1992. DNA damage and mutation in human cells exposed to nitric oxide. *Proc. Natl. Acad. Sci. USA.* 89:3030–3034.
29. Wink, D.A., Y. Osawa, J.F. Darbyshire, C.R. Jones, S.C. Eshenaur, and R.W. Nims. 1993. Inhibition of cytochromes P450 by nitric oxide and a nitric oxide-releasing agent. *Arch. Biochem. Biophys.* 300:115–123.
30. Laval, F., and D.A. Wink. 1994. Inhibition by nitric oxide of the repair protein, O6-methylguanine-DNA-methyltransferase. *Carcinogenesis.* 15:443–447.
31. Stamler, J.S., I.S. Simon, J.A. Osborne, M.E. Mullins, O. Jaraki, T. Michel, D.J. Singel, and J. Loscalzo. 1992. S-Nitrosilation of proteins with nitric oxide: synthesis and characterization of biologically active compounds. *Proc. Natl. Acad. Sci. USA.* 89:444–448.
32. Radi, R., J.S. Beckman, K.M. Bush, and B.A. Freeman. 1991. Peroxynitrite-induced membrane lipid peroxidation: the cytotoxic potential of superoxide and nitric oxide. *Arch. Biochem. Biophys.* 288:481–487.
33. Lancaster, J.R., and J.B. Hibbs. 1990. EPR demonstration of iron-nitrosyl complex formation by cytotoxic activated macrophages. *Proc. Natl. Acad. Sci. USA.* 87:1223–1227.
34. Drapier, J.C., H. Hirling, J. Wietzerbin, P. Kaddy, and L.C. Kuhn. 1993. Biosynthesis of nitric oxide activates iron regulatory factor in macrophages. *EMBO (Eur. Mol. Biol. Organ.) J.* 12:3643–3649.
35. Wink, D.A., and J. Laval. 1994. The Fpg protein, a DNA repair enzyme, is inhibited by the biomediator nitric oxide *in vitro* and *in vivo*. *Carcinogenesis.* 15:2125–2129.
36. Imlay, J.A., S.M. Chin, and S. Linn. 1988. Toxic DNA damage by hydrogen peroxide through the Fenton reaction in vivo and in vitro. *Science (Wash. DC).* 240:640–642.
37. Borchman, D., O.P. Lamba, S. Salmassi, M. Lou, and M.C. Yappert. 1992. The dual effect of oxidation on lipid bilayer structure. *Lipids.* 27:261–265.
38. Salgo, M.G., F.P. Corongiu, and A. Sevanian. 1992. Peroxi-

dation and phospholipase A2 hydrolytic susceptibility of liposomes consisting of mixed species of phosphatidylcholine and phosphatidylethanolamine. *Biochim. Biophys. Acta.* 1127:131–140.

39. Meister, A., and M.A. Anderson. 1983. Glutathione. *Annu. Rev. Biochem.* 52:711–760.
40. Costerton, J.W., J.M. Ingram, and K.J. Cheng. 1974. Structure and function of the cell envelope of gram-negative bacteria. *Bacteriol. Rev.* 38:87–110.
41. Hassan, M.H., and I. Fridovich. 1977. Regulation of the synthesis of superoxide dismutase in *Escherichia coli*. *J. Biol. Chem.* 252:7667–7672.
42. Halliwell, G., and J.M.C. Gutteridge. 1989. Free Radicals in Biology and Medicine. Clarendon Press, Oxford, UK. pp. 131–133.
43. Marletta, M.A., M.A. Tayeh, and J.M. Hevel. 1990. Unraveling the biological significance of nitric oxide. *Biofactors.* 2: 219–225.
44. Lin, J.Y., and K. Chadee. 1992. Macrophage cytotoxicity against *Entamoeba histolytica* trophozoites is mediated by nitric oxide from L-arginine. *J. Immunol.* 148:3999–4005.
45. Li, Y., A. Severn, M.V. Rogers, R.M. Palmer, S. Moncada, and F.Y. Liew. 1992. Catalase inhibits nitric oxide synthesis and the killing of intracellular *Leishmania major* in murine macrophages. *Eur. J. Immunol.* 22:441–446.
46. Hausladen, A., and I. Fridovich. 1994. Superoxide and peroxynitrite inactivate aconitases, but nitric oxide does not. *J. Biol. Chem.* 269:29405–29408.
47. Castro, L., M. Rodrigue, and R. Radi. 1994. Aconitase is readily inactivated by peroxynitrite, but not by its precursor, nitric oxide. *J. Biol. Chem.* 269–29409–29415.